Morphology-dependent electrical transport in textured ultra-thin Al films on Si

D.K. Aswal, N. Joshi, A.K. Debnath, K.P. Muthe, S.K. Gupta, J.V. Yakhmi, D. Vuillaume

Morphology-dependent electric transport in textured ultrathin Al films grown on Si

Cite as: J. Appl. Phys. **98**, 026103 (2005); https://doi.org/10.1063/1.1977188
Submitted: 21 February 2005 • Accepted: 01 June 2005 • Published Online: 19 July 2005

D. K. Aswal, Niraj Joshi, A. K. Debnath, et al.

Morphology-dependent electric transport in textured ultrathin Al films grown on Si

D. K. Aswal,[a] Niraj Joshi, A. K. Debnath, K. P. Muthe, S. K. Gupta, and J. V. Yakhmi
Technical Physics and Prototype Engineering Division, Bhabha Atomic Research Center, Modular Laboratory, Trombay, Mumbai 400 085, India

Dominique Vuillaume
Institut d'Electronique, Microelectronique et Nanotechnologie—Centre National de la Recherche Scientifique (CNRS) Molecular Nanostructures and Devices Group, BP60069, avenue Poincare, Villeneuve d'Ascq, F-59652 Cedex, France

(Received 21 February 2005; accepted 1 June 2005; published online 19 July 2005)

The thickness and temperature dependence of the electrical resistivity of the (111) textured ultrathin aluminum metal films grown on (111) Si substrates using molecular-beam epitaxy have been investigated. For films with thickness <50 nm, the room-temperature value of resistivity—contrary to the predictions of existing theoretical models—is found to increase monotonically with thickness. In addition, the temperature dependence of these films exhibited a metal-to-insulator transition at ~ 110 K. The studies of films using atomic force microscopy, x-ray photoelectron spectroscopy, and x-ray diffraction revealed that the observed anomalous thickness and temperature dependence of resistivity arise due to the formation of two-dimensional network of Al islands, and the low-temperature electric transport of such films could be explained using variable range hopping conduction. © *2005 American Institute of Physics*. [DOI: 10.1063/1.1977188]

Ultrathin films, thickness (t) <50 nm, of metals, e.g., Al, Au, Pd, etc., are of technological importance for nanotechnology. In particular, ultrathin Al films are considered to be a potential candidate as a buffer layer for Ag or Cu metallization in futuristic ultralarge-scale integration (ULSI) or gigascale integration (GSI) technology.[1–5] However, at such a low t (<50 nm) the electrical resistivity of Al is expected to be much higher than that of the bulk value due to various known effects. (i) External size effect: as t of the film becomes smaller than the mean free path (λ) of the electrons, the electrons are scattered at the external surface, which results in an increase in the film resistivity. This effect in metallic thin films was developed by Fuschs and extended by Sondheimer (known as FS theory).[6] (ii) Internal size effect: the internal size effect theory, developed by Mayadas *et al.*,[7] takes into account the electron scattering at the grain boundaries. (iii) Electron scattering at impurities, vacancies, and dislocations as thin films are more susceptible to the formation of these defects.

Most of the previous works on ultrathin Al films were done on polycrystalline samples deposited on SiO_2 or glass at ambient temperature.[8,9] For such films, the t dependence of resistivity was found to be in agreement with the above-mentioned theories. In this communication, we show that the electrical properties of textured ultrathin Al films grown on technologically important Si substrates are not in agreement with existing theoretical models. We have observed that textured ultrathin Al films grow via the Volmer-Weber growth mechanism, which leads to the formation of a two-dimensional network of Al islands, and low-temperature electrical transport in these films is best described by variable range hopping (VRH) conduction.

Ultrathin Al films of different t in the range of 10–200 nm were grown in a molecular-beam epitaxy (MBE) system (RIBER model EVA 32), and the details of the MBE system, substrate preparation, and deposition process are discussed in our recent papers.[3–5] The film deposition on chemically cleaned and vacuum baked Si (111) substrates ($\rho > 1\ \Omega$ cm) were carried out at 250 °C. The evaporation source employed was an effusion cell loaded with 99.999% pure Al. The base vacuum during the depositions was better than 10^{-9} torr. For the measurement of deposition rate, the pressure (p) of the material in substrate position was measured using a flux gauge, and the flux was calculated using the relation $F = 3.52 \times 10^{22}\ P/\sqrt{MT}$ molecules/cm^2 s, where p is in torr, M is the molecular weight of Al, and T (1473 K) is the temperature of the effusion cell. The deposition rate was found to be ~ 0.15 Å/s. After deposition, Al films were transferred without breaking vacuum to an analysis chamber for x-ray photoelectron spectroscopy (XPS) measurements. XPS spectra were recorded using Mg Kα (1253.6 eV) source and a made analyzer computer (MAC)-2 electron analyzer. The binding-energy scale was calibrated to Au $4f_{7/2}$ line of 83.95 eV.

The film texture was assessed by x-ray-diffraction measurements. The surface morphologies of the Al films were recorded *ex situ* under ambient conditions using a scanning probe microscope (SPM, model Solver P47) in noncontact mode.[10] The electrical resistivity of the Al films was measured by linear four-probe method in the temperature range of 300–30 K using a close cycle Helium cryostat.

The recorded x-ray-diffraction (XRD) patterns showed that Al films, irrespective of the t of films, are highly (111)

[a]Author to whom correspondence should be addressed; present address: IEMN-CNRS, BP60069, avenue Poincare, Villeneuve d'Ascq, F-59652 Cedex, France; FAX: +91-22-550-5151; electronic mail: dkaswal@yahoo.com

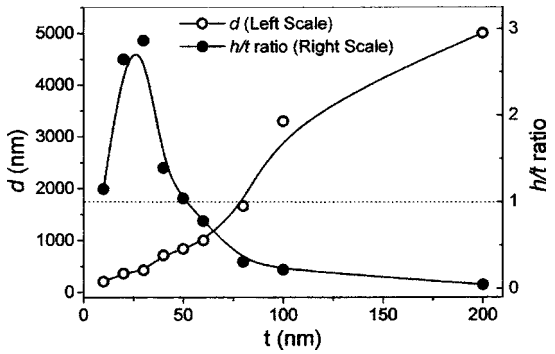

FIG. 1. Thickness (t) dependence of average grain size (d) and average surface roughness (h) to t ratio, i.e., h/t ratio, measured for Al thin films. The solid lines are obtained by B-spline fitting of the data points and are provided as guide to the eye.

oriented. The atomic force microscopy (AFM) images depicting the morphology of Al thin films of different thicknesses have been recorded. The AFM images have been quantified by recording the height profiles across the length of the images, as described in our earlier paper.[10] This quantification provides information on the average grain size (d) and average surface roughness (h). The obtained results on t dependence of d and h/t ratio are plotted in Fig. 1. From Fig. 1, the major inferences drawn are as follows. (i) The films grow via three-dimensional (3D)-island Volmer-Weber growth mechanism. (ii) The d increases monotonically up to a thickness of 100 nm and above that the films become continuous across the substrates. (iii) An h/t ratio >1 implies that the films are very rough. Thus, the data of Fig. 1 indicate that for $t \leqslant 50$ nm the isolated islands form a random two-dimensional network, which is also apparent from Fig. 1. The h/t ratio becomes less than 1 for $t \geqslant 60$ nm, which indicates that the coalescence of islands begins for a thickness of 60 nm. The h/t ratio for film thickness of 100 nm is only 0.046, indicating that all the grains are fused together and the resultant film is continuous.

The core-level Al-2p and Si-2p XPS spectra recorded for Al thin films of different thicknesses are shown in Fig. 2. It is seen that Al is mainly in the metallic state (corresponding to a peak at 72.4 eV); however, the presence of a faint peak at 74.8 eV reveals the formation of oxide, which indicates strong affinity of Al towards the residual oxygen present in the growth chamber.[3] In addition, a peak corresponding to Si

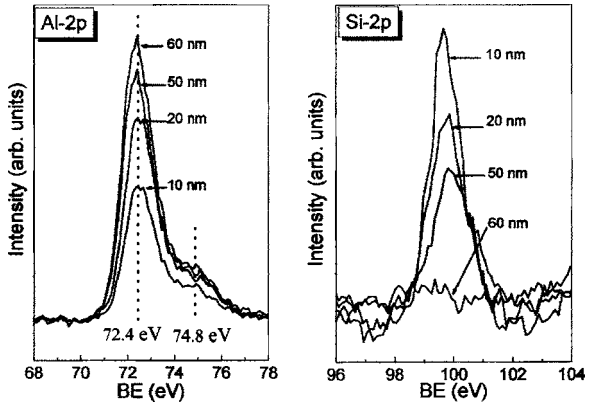

FIG. 2. Core-level Al-2p and Si-2p spectra recorded for Al thin films of different thicknesses. The intensity of Si peak decreases with increasing film thickness.

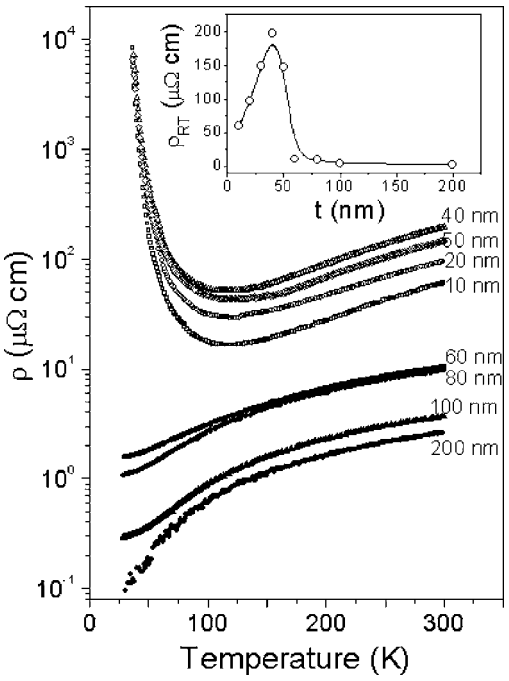

FIG. 3. Temperature dependence of ρ recorded for Al films of different thicknesses. Note the metal-to-insulator transition for films with $t \leqslant 50$ nm at around 110 K. Inset: room-temperature resistivity (ρ_{RT}) of Al thin films as a function of film thickness. The solid line is obtained by B-spline fitting of the data points and is provided as guide to the eye.

is observed for t range of 10–50 nm, though the intensity monotonically decreases and becomes zero for the 60-nm film. The observation of a large Si peak is quite interesting considering the facts that (i) Al does not form silicide as other (Fe, Ti, V, etc.) metals and Si has very low solubility in Al (Refs. 11 and 12) and (ii) XPS is a surface sensitive technique with a sampling depth of 3 nm.[13] Since the minimum t of our films is 10 nm, therefore the XPS signals of Si are attributed to originate from the interisland regions of Al films. The Si peak vanishes for $t \geqslant 60$ nm, and this is expected as Al islands coalesce. Thus, the XPS data provide an additional support to the AFM analyses on t-dependent island-type growth and coalescence of Al films.

The measured room-temperature resistivity (ρ_{RT}) of (111)-oriented Al thin films plotted against t is shown in the inset of Fig. 3. The ρ_{RT} value of the 10-nm films is 59.9 $\mu\Omega$ cm, which increases monotonically up to a value of 196.6 $\mu\Omega$ cm as t increases to 40 nm. The ρ_{RT} is found to decrease for $t > 40$ nm. It may be noted that ρ_{RT} drops by an order of magnitude as t increases from 50 to 60 nm. The bulk value of ρ_{RT} (2.69 $\mu\Omega$ cm) is obtained for a t value of 200 nm. We analyze this ρ_{RT} vs t data using the framework of existing models.[6,7,14] As discussed earlier, the larger electrical resistivity of metal thin films compared to that of the bulk value arise due to external size effect, internal size effect, and electron scattering due to impurities, vacancies, and dislocations. Dobierzewska-Mozrzymas and Warkusz[14] considered all these factors and derived the following theoretical relation for the metallic thin films:

$$\rho = \rho_b + \rho_d + \rho_t. \tag{1}$$

In this equation, ρ_b is the bulk value of resistivity and takes-into account impurities, vacancies, and dislocations, ρ_d is the

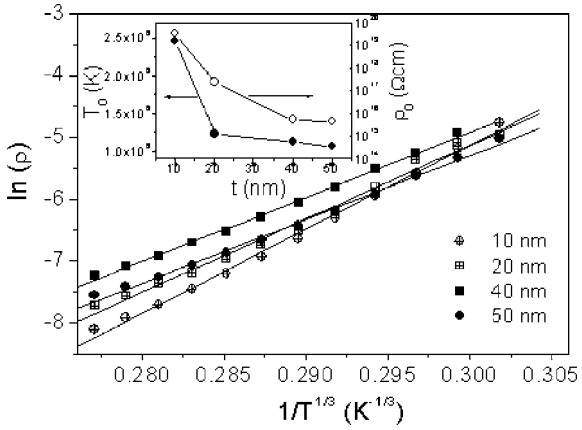

FIG. 4. The data of the insulating region in Fig. 3 for films with $t \leqslant 50$ nm replotted as $\ln \rho$ vs $T^{-1/3}$. The straight lines are linear fit to the data. The inset shows the variation of parameters T_0 and ρ_0 with film thickness.

resistivity that depends on the grain diameter (d) via the relation $\rho_D = 3\lambda R\rho_b / 2d(1-R)$ (where λ is the electron mean free path, R is the grain-boundary scattering coefficient), and ρ_t is the resistivity term that depends on t via $\rho_t = 3\lambda(1-f)\rho_b / 8t$ (where f is the fraction of electrons specularly scattered at the external surface).

According to Eq. (1), the ρ_{RT} should decrease with increasing t as well as d. In the present case, this theory appears to be valid for t in the range between 50 and 200 nm, as ρ_{RT} decreases with increasing t. However, for t in the range of 10–40 nm, contrary to the prediction of Eq. (1), the ρ_{RT} increases with t despite of the fact that in this range both t and d increase. Thus, the mechanism of electrical transport in this t range appears to be radically different. As we have discussed earlier, the growth morphology of films having $t \leqslant 50$ nm consists of two-dimensional (2D) network of Al islands. Moreover, as the XPS data of Fig. 2 suggest, the grain boundaries of such Al islands are covered with aluminum oxide. These results indicate that the charge carriers are localized within grains and, therefore, transport of charge carriers is likely to be dominated by the hopping mechanism. The best way to test the hopping conduction is to measure the temperature dependence of ρ, and the results are shown in Fig. 3. It is evident that all the ρ-T curves for films with t in the range of 10–50 nm exhibit a metal-to-insulator (M-I) transition around 110 K. If the charge transport takes place via the hopping mechanism, then the insulating part should obey the theoretical prediction of 2D VRH conduction,[15] i.e.,

$$\rho = \rho_0 \exp(T_0/T)^{1/3}. \tag{2}$$

In order to test the validity of Eq. (2), the low-temperature data are plotted as $\ln \rho$ vs $(1/T)^{1/3}$, and is shown in Fig. 4. A linear fit of the data suggests that charge transport takes place via 2D VRH. The parameters T_0 and ρ_0, determined, respectively, from the slope and intercept on the Y axis of the linear fit, are plotted as a function of t in the inset of Fig. 4. A decrease in both the parameters indicates that charge localization becomes weaker as t increases. This might be related to an increase in island diameter (see Fig. 1) as the surface-to-volume ratio decreases with increasing diameter, and the surface oxide layer contributes to the localization. This behavior, however, contradicts the increase in ρ_{RT} with t as well as d. This is not surprising as at high temperatures all the films show a metallic behavior, indicating a different conduction mechanism. These results reveal that the mechanism of charge transport in these films is temperature dependent, and requires further investigations to understand the anomalous behaviors. It may be noted that the M-I transition observed in the present case, as one may suspect, is not due to the interdiffusion of Si into Al. The solubility of Si in Al is about 1% at an annealing temperature of 500 °C.[16,17] But our processing temperature was 250 °C, hence solubility of Si in the films would be much lower. If the presence of Si or the interfacial reaction is considered solely responsible for the M-I transition, then the M-I transition temperature should systematically shift to lower temperature with increasing film thickness as due to diffusion limitation less Si would be incorporated in thicker films (this is supported by the XPS data of Fig. 2). But it is seen in Fig. 3 that the M-I transition temperature remains around 110 K for all thicknesses (10–50 nm). Further absence of M-I transition for films of 60 nm thickness coincides with the absence of grain boundaries for this thickness (as discussed above), indicating that growth morphology is responsible for the M-I transition.

In conclusion, textured ultrathin Al films ($t \leqslant 50$ nm) form a random two-dimensional network of islands on Si (111) substrate via the Volmer-Weber mechanism. The electrical resistivity of such films cannot be accounted by the known existing models for thin films. It has been shown that the low-temperature electrical transport in these films obeys a 2D variable range hopping conduction mechanism.

ACKNOWLEDGMENT

This work was supported by the Indo-French Centre for the Promotion of Advanced Research (IFCPAR) through Project No. 3000-IT-I.

[1] S. P. Murarka, Mater. Sci. Eng., R. **19**, 87 (1997).
[2] Y. Wang and T. L. Alford, Appl. Phys. Lett. **74**, 52 (1999).
[3] A. K. Debnath, N. Joshi, K. P. Muthe, J. C. Vyas, D. K. Aswal, S. K. Gupta, and J. V. Yakhmi, Appl. Surf. Sci. **243**, 218 (2005).
[4] D. K. Aswal, A. K. Debnath, N. Joshi, K. P. Muthe, S. K. Gupta, and J. V. Yakhmi, *International Conference on Advances in Surface Treatment: Research and Applications (ASTRA 2003), Hyderabad, India, 3–6 November 2003* (unpublished).
[5] D. K. Aswal, K. P. Muthe, N. Joshi, A. K. Debnath, S. K. Gupta, and J. V. Yakhmi, J. Cryst. Growth **256**, 201 (2003).
[6] E. H. Sondheimer, Adv. Phys. **1**, 1 (1952).
[7] A. F. Mayadas, M. Shatzkes, and J. F. Janak, Appl. Phys. Lett. **14**, 343 (1969).
[8] J. W. C. de Vries, Thin Solid Films **167**, 25 (1988).
[9] J. Gogl, J. Vancea, and H. Hoffmann, J. Phys.: Condens. Matter **2**, 1795 (1990).
[10] D. K. Aswal, K. P. Muthe, S. Tawde, S. Chodhury, N. Bagkar, A. Singh, S. K. Gupta, and J. V. Yakhmi, J. Cryst. Growth **236**, 661 (2002).
[11] J. L. Murray and A. J. McAlister, Bull. Alloy Phase Diagrams **5**, 74 (1984).
[12] *Thin Films Interdiffusion and Reactions*, edited by J. M. Poate, K. N. Tu, and J. W. Mayer (Wiley, New York, 1978), p. 380.
[13] D. Briggs and M. P. Seah, *Practical Surface Analysis by Auger and X-ray Photoelectron Spectroscopy* (Wiley, New York, 1983).
[14] E. Dobierzewska-Mozrzymas and F. Warkusz, Thin Solid Films **43**, 267 (1977).
[15] N. F. Mott, *Metal-Insulator Transitions* (Taylor & Francis, London, 1990).
[16] J. O. McCaldin and H. Sankur, Appl. Phys. Lett. **19**, 524 (1971).
[17] R. L. Boatright and J. O. McCaldin, J. Appl. Phys. **47**, 2260 (1976).